

## **Sequence-stratigraphic interpretation of structurally controlled deposition: Middle Miocene Kareem Formation, southwestern Gulf of Suez, Egypt**

Ahmed I.M. Abd El-Naby, Hussam Ghanem, Mohamed Boukhary,  
Mohamed Abd El-Aal, Sebastian Lüning and Jochen Kuss

### **ABSTRACT**

The structural evolution and sequence-stratigraphic architecture of the syn-rift Middle Miocene (Langhian) Kareem Formation were studied in the Western Sub-Basin (WSB) of the Gulf of Suez, Egypt. Biostratigraphic data, facies interpretations, and log data from thirteen wells were used to construct six tectono-sedimentary scenarios and lithofacies-distribution maps, which illustrate the paleogeography during six systems tracts. Abrupt thickness and facies changes reflect deep basins and adjacent high-relief areas created by differential fault-block movements. Within the WSB seven individual fault blocks record complex, tectonically controlled deposition of the Kareem Formation, which we subdivide into two third-order sequences. Earlier tectonic interpretations, facies analysis, and stratigraphic correlations from individual fault blocks were used to interpret the varying depositional settings during six systems tracts and, as a consequence, to discern the structural evolution of the WSB during the Middle Miocene.

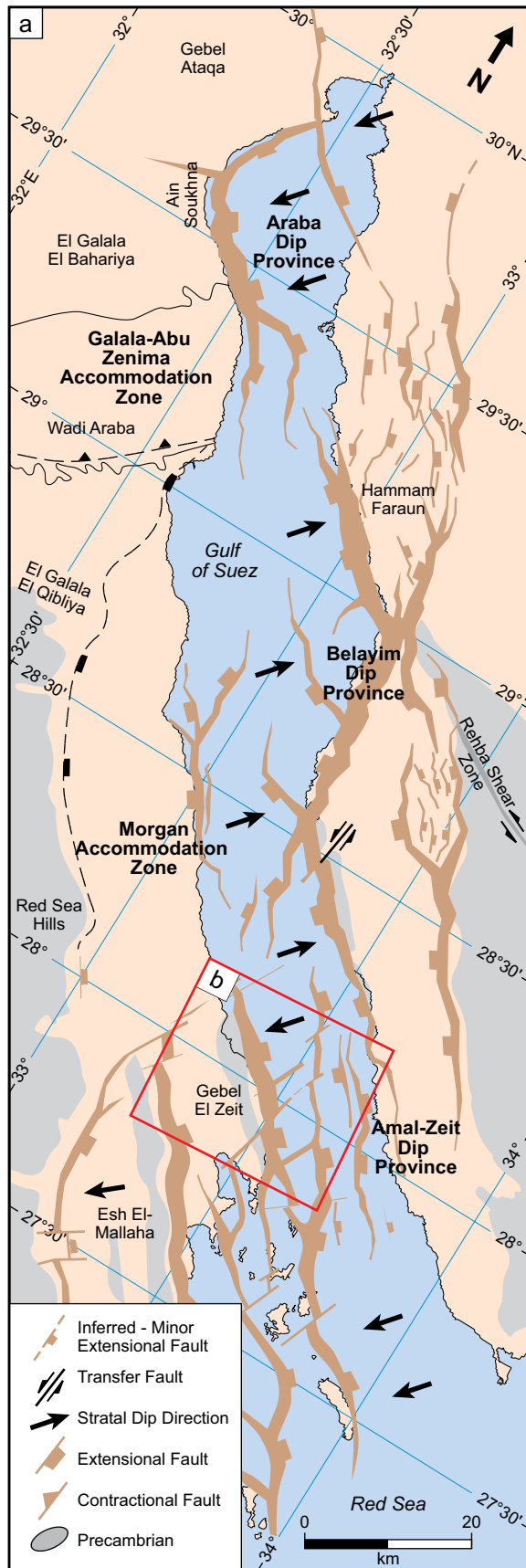
### **INTRODUCTION**

The relationships between tectonics and sedimentation in extensional settings reveal the role of fault evolution and interaction in controlling the deposition, dispersal, and architecture of syn-extensional sediments (Gawthorpe et al., 1990, 1994; Gawthorpe and Hurst, 1993; Hardy et al., 1994; Gupta et al., 1999; Young et al., 2000; Winn et al., 2001; Jackson et al., 2005; Herkat and Guiraud, 2006; Khalil and McClay, 2008). Structural and sedimentological studies of active rift basins show that abrupt thickness and facies changes as well as slip rates along normal faults are the major factors influencing the spatial distribution and architecture of depositional systems adjacent to the fault zones (Seger and Alexander, 1993; Gawthorpe and Leeder, 2000; Leeder et al., 2002; Jackson et al., 2005; Herkat and Guiraud, 2006; Leppard and Gawthorpe, 2006; Khalil and McClay, 2008). In the southwestern part of the Gulf of Suez, syn-rift clastics of the Kareem Formation formed coarse-grained fan deltas and submarine fans at sediment-input points along the coastal plain. The aim of this paper is to illustrate the structural control on sequence stratigraphy of the syn-rift Middle Miocene (Langhian) Kareem Formation, and the tectonic influence on the location of major sediment-input points in the southwestern part of the Gulf of Suez.

### **GEOLOGIC SETTING**

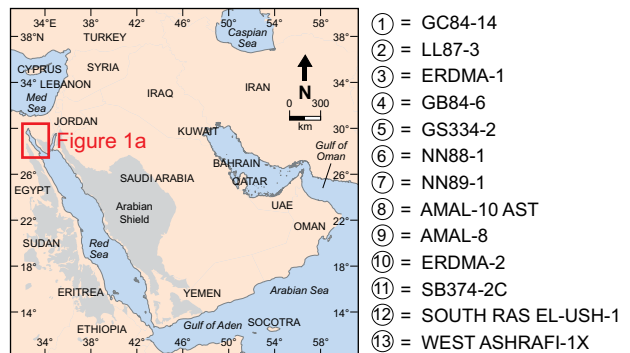
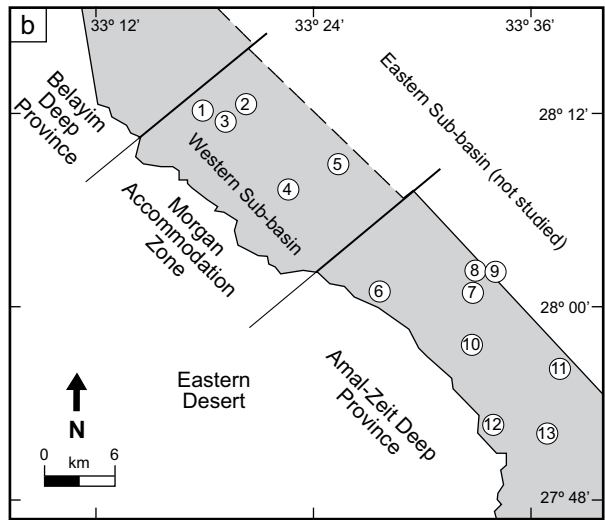
The Gulf of Suez is a Neogene continental rift system that developed by the separation of the African and Arabian plates in Late Oligocene – Early Miocene time. Geomorphologically it represents a rejuvenated, slightly arcuate NW-SE topographic depression, known as the Clysmic Gulf. It extends northwestward from 27°30'N to 30°00'N. Its width varies from about 50 km at its northern end to about 90 km at its southern end where it merges with the Red Sea (Bosworth and McClay, 2001, Figure 1). The Gulf of Suez is dissected by a complex pattern of faults: N-S to NNE-SSW as well as E-W trending normal faults at the rift borders and within the rift basin, and NE-trending strike-slip faults crossing the Gulf basin (Abd El-Naby et al., 2009). The interaction of these major fault systems resulted in a complex structural pattern consisting of numerous horsts and grabens with variable relief and dimensions.

The Gulf of Suez is subdivided into three structural provinces according to their structural settings and regional dip directions: the northern Araba dip province (SW dips), the central Belayim dip



province (NE dips), and the southern Amal-Zeit dip province (SW dips, Figure 1). These provinces are separated by two NE-trending accommodation zones: the Galala-Abu Zenima Accommodation zone (GAZAZ) in the north, and the Morgan Accommodation zone (MAZ) in the south. The study area of the WSB (about 60 km long and 12.5 km wide) covers the MAZ and the northern part of the Amal-Zeit dip province (AZP, Figure 1).

Based on surface and subsurface data, the stratigraphic succession of the Gulf of Suez can be subdivided into three depositional units (Figure 2, see Abd El-Naby et al., 2009). The pre-rift units include Proterozoic basement rocks and Paleozoic to Upper Eocene sediments. These formations are important as source and reservoir rocks. The Upper Oligocene and Miocene syn-rift units contain source, reservoir and seal lithologies, as well as volcanic rocks. The post-rift units are of Pliocene to Pleistocene age.



- ① = GC84-14
- ② = LL87-3
- ③ = ERDMA-1
- ④ = GB84-6
- ⑤ = GS334-2
- ⑥ = NN88-1
- ⑦ = NN89-1
- ⑧ = AMAL-10 AST
- ⑨ = AMAL-8
- ⑩ = ERDMA-2
- ⑪ = SB374-2C
- ⑫ = SOUTH RAS EL-USH-1
- ⑬ = WEST ASHRAFI-1X

**Figure 1: Tectonic map of the Gulf of Suez Rift (modified after Bosworth and McClay, 2001; Abd El-Naby et al., 2009). The study area (rectangle, including location of the studied 13 wells) is located in the northern Amal-Zeit dip provinces and the Morgan Accommodation Zone.**

## MATERIALS AND METHODS

Our sequence-stratigraphic analysis of the Kareem Formation is based mainly on the interpretation of key chronostratigraphic surfaces and systems tracts identified in 13 wells located in the study area of the Western Sub-Basin (WSB, Figure 1). We utilized lithologic interpretations, cuttings, logs (Gamma Ray [GR], Resistivity, Sonic, Density, and Neutron), planktonic foraminifer abundances (PFA), and benthonic/planktonic (B/P) ratios to detect paleobathymetric and environmental variations during deposition. Our approach for defining the key surfaces and systems tracts is based on Emery and Myers (1996), Posamentier and Allen (1999), and Rider (2004).

Tectono-sedimentary models and lithofacies distribution maps were constructed for six systems tracts interpreted in the Kareem Formation. Facies analysis allows us to illustrate the effect of synrift cross faults and fault-block movement on Kareem sedimentation (Figures 2 and 3).

## DESCRIPTION OF KEY SURFACES AND SYSTEMS TRACTS

The general description of both third-order sequences and six system tracts of the Kareem Formation can be summarized as follows. Most sequence boundaries (SBs) are marked by an abrupt decrease in GR and PFA (Figure 4). The lowstand systems tract (LST) sediments above each are characterized by blocky GR, relatively high resistivity, low velocity, and high to low density and neutron log responses, along with decreasing PFA and an increasing B/P ratio. The lithology of these sediments consists mainly of anhydrites and sandstones with

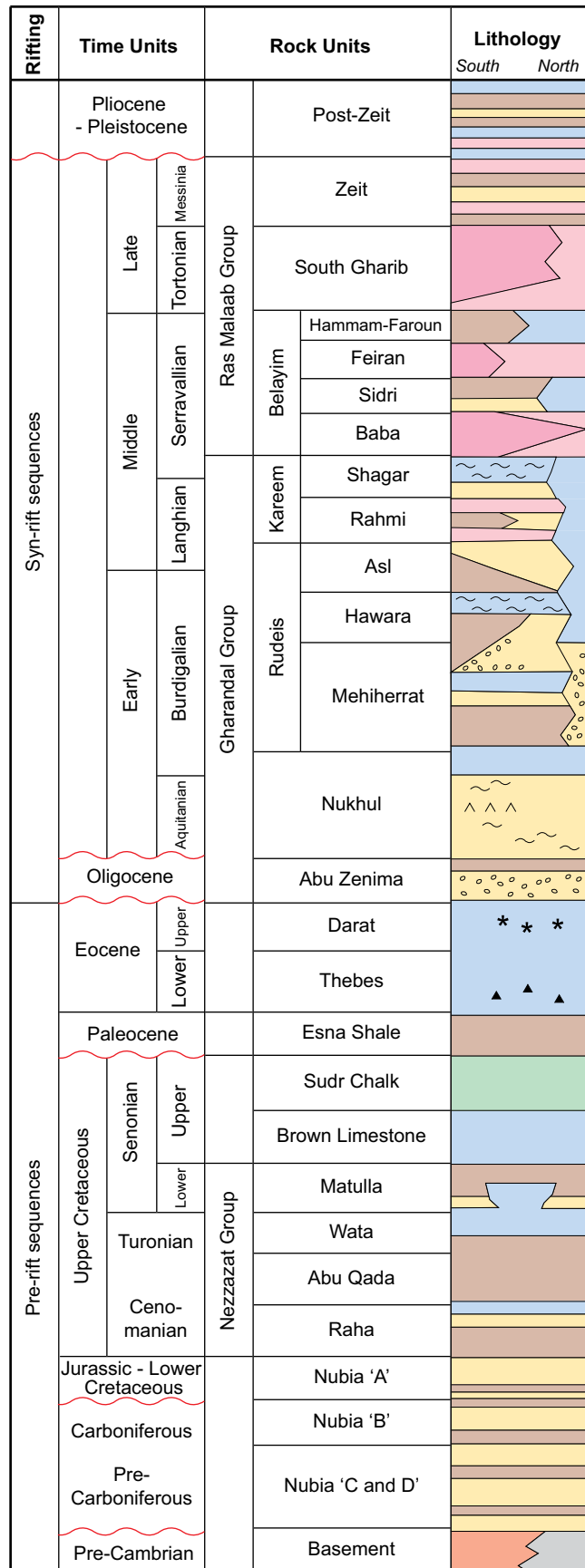
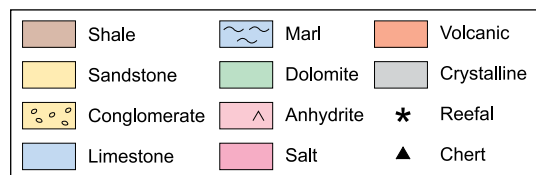


Figure 2: Stratigraphic column of the Gulf of Suez (modified after Schlumberger, 1995; Abd El-Naby et al., 2009).

few argillaceous limestones and calcareous shales. Conglomerate clasts of mainly quartz with few feldspar grains, plus granite, carbonate, and shale, are also present.

Transgressive surfaces (TS) are delineated by a gradual upward increase in GR and PFA, whereas the transgressive surface of erosion (TSE) is characterized by an abrupt increase in GR and PFA. The transgressive systems tracts (TST) are characterized by an upward increase in GR (“dirtying-upward”) and PFA coupled with decreasing B/P ratios, moderate to low resistivity, and high to low velocity. These sediments also are marked by high to low density and high to moderate neutron responses. The TSTs are composed mainly of calcareous shales, argillaceous limestones, and sandstones with few siltstones. Compared with the LST deposits, the TST sediments contain smaller clasts of quartz, shale, and carbonate as well as fewer feldspar grains.

The maximum flooding surfaces (MFS) coincide with peaks in GR and PFA. In contrast to the TSTs, the highstand systems tracts (HST) are marked by a gradual upward decrease in GR (“cleaning-upward” trend) and PFA associated with increasing B/P ratios, moderate to low resistivity, high to low velocity, moderate to low density, and high to moderate neutron readings. These sediments consist of sandstones, calcareous shales, and argillaceous limestone intercalations with clasts of mainly quartz, plus shale, carbonate, and feldspar grains.

Marine sediments are absent on Fault Block (FB) V (Figures 8 to 13), while only thin fluvial sandstones (facies type C) are deposited on this fault block (Figure 3). These sandstones could not be referred to one of the defined systems tracts.

The absence of marine sediments in the Amal-Zeit Province (AZP) at ERDMA-2 and SB374-2C wells (Figures 8 to 13) reflects a structurally controlled elevation of FB V above sea level. Furthermore, Early – Middle Miocene sediments (Kareem, Rudeis and Nukhul formations) are absent at SB374-2C well (see below for more discussion).

Important characteristics, including thickness, lithology, log trends, foraminiferal trends, and depositional environments of all systems tracts of the two third-order genetic sequences of the Kareem Formation are summarized in Figure 5. Moreover, we summarize the individual tectonic block movements and thickness variations during deposition of all these systems tracts (Figure 6).

### DESCRIPTION OF FAULT BLOCKS IN THE WESTERN SUB-BASIN (WSB)

Seven fault blocks (FB I to FB VI, including FB IVa and FB IVb) are defined in a tentative tectono-sedimentary model in the study area (Figure 7). The location of these fault blocks along the WSB can be compared to the two-way time-structure contour

Lithology	Petrography and fossil contents	Depositional Environments
Sandstones (A)	Coarse grains, large pebbles, angular to subrounded, poorly sorted. Fe-oxides and carbonate cements. Subrounded to angular clasts of mainly quartz, feldspars, granite, carbonate, mica flakes and shale. Few planktonic and benthonic foraminifers.	Fan delta
Sandstones (B)	Coarse to medium grains, smaller pebbles, subrounded to angular, moderately to poorly sorted. Fe-oxides and carbonate cements. Smaller subrounded to angular clasts of similar composition as fan delta. Few planktonic and benthonic foraminifers.	Submarine fan
Sandstones (C)	Coarse to medium grain, large pebbles, subangular to angular, poorly to moderately sorted. Fe-oxides and carbonate cements. Unfossiliferous.	Fluvial
Shales	Grey-dark grey, flaky, silty fissile, highly calcareous, locally grading to argillaceous limestones, highly fossiliferous (rich in planktonic foraminifers and nannofossils with few benthonic foraminifers).	Middle neritic to upper bathyal
Limestones	White to pale brown, cryptocrystalline, very fine, argillaceous, highly sandy, locally cherty and anhydritic. Highly fossiliferous (rich in planktonic foraminifers and nannofossils with few benthonic foraminifers).	Lagoonal to upper bathyal
Anhydrites	Milky white, milky grey white, white, micro- to cryptocrystalline, occasionally calcareous.	Lagoonal

**Figure 3: Characteristics of the six major lithologies of the Kareem Formation in the study area and general facies interpretations based on cuttings and core description (with additional remarks from the original descriptions of the composite logs).**

map of top Kareem Formation (Abd El-Naby et al., 2009). The blocks are bounded by six major cross faults with near-orthogonal orientations to the NW-SE oriented clysmic faults (Figure 7). The rates of vertical and horizontal movements along these cross faults varied, resulting in differential subsidence rates and rotations of the individual fault blocks. Subsidence rates of the individual fault blocks were deduced from thickness variations of the individual systems tracts within FB I to FB VI (Figure 6; see also Young et al., 2000; Winn et al., 2001; Jackson et al., 2005; Herkat and Guiraud, 2006; Khalil and McClay, 2008).

FB I is located at the northern boundary of the MAZ (Figure 7) and characterized by right-lateral transtensional movements and low to moderate subsidence rates (Figure 6). FB II is located in the MAZ southeast to the structurally higher FB I (Figure 7). Right-lateral transtensional movements of FB II were accompanied by low to moderate subsidence rates (Figure 6). FB I and FB II reacted as one fault block during during deposition of LST2 (see below for more discussion). FB III represents the structurally lowest block in the WSB (Figure 7) with maximum subsidence rates indicated by high sediment accumulation. It forms the southeastern boundary of the MAZ and is characterized by both right-lateral and left-lateral transtensional movements (Figure 6). FB IV is located at the northeastern part of the AZP (Figure 7) and underwent left-lateral transtensional movements associated with low to moderate subsidence rates (Figure 6). This fault block was affected by a NW-oriented fault (Figures 8 to 13), which subdivided it into two sub-blocks (details are addressed below). FB V remained in a structurally high position (above 90 sea level) during the entire time of Kareem deposition (Figures 7 to 13). FB VI, located at the southernmost part of the WSB (in the AZP), experienced left-lateral transtensional movements, coupled with low to high subsidence rates (Figure 6).

## **SEQUENCE STRATIGRAPHY AND FACIES ANALYSIS OF THE KAREEM FORMATION**

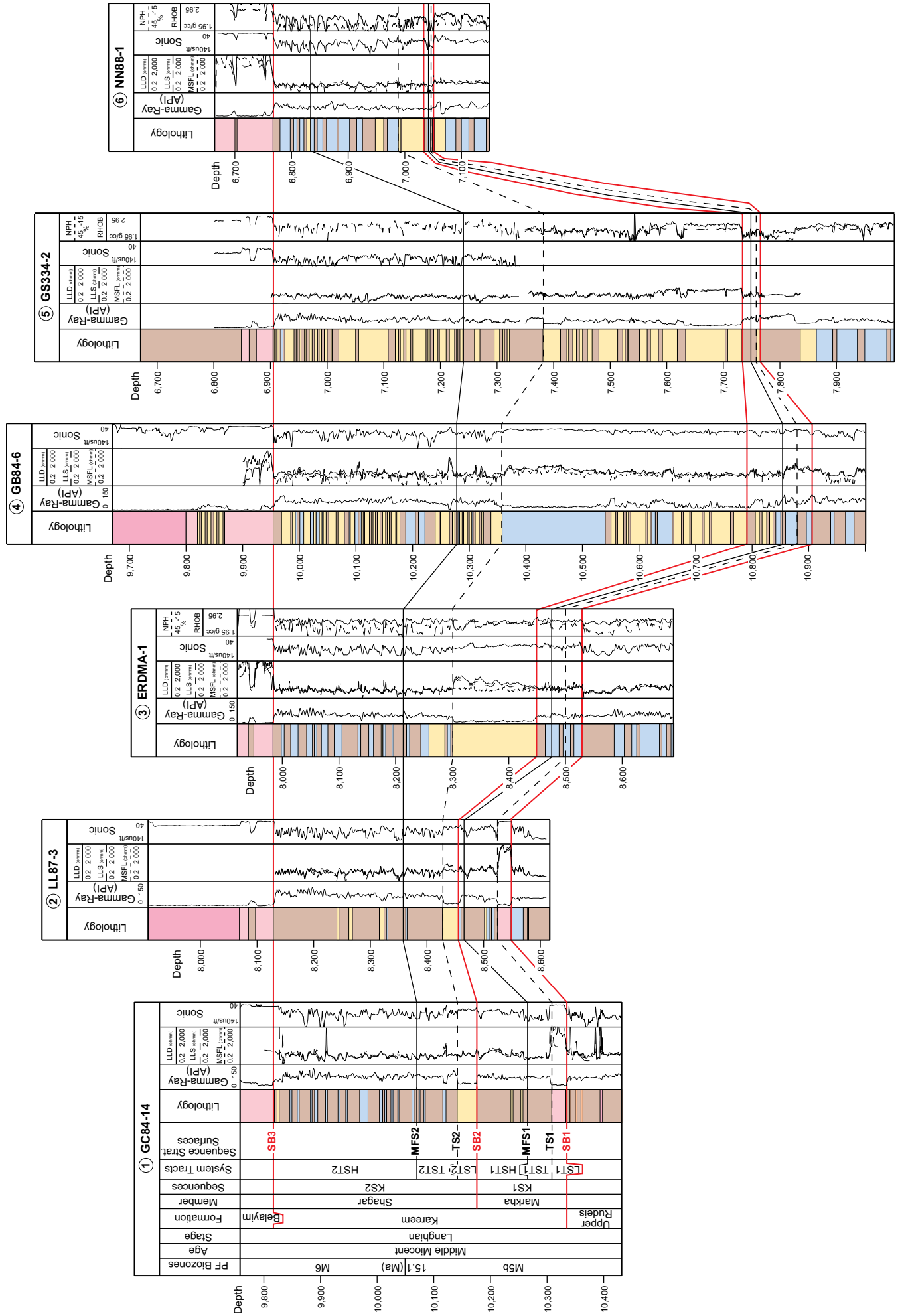
Our third-order sequences of the Kareem Formation, KS1 (Kareem sequence 1) and KS2 (Kareem sequence 2), can be contrasted with sequences S40 and S50 of Dolson et al. (1996), Ramzy et al. (1996), and Krebs et al. (1997), which are widely distributed in the Gulf of Suez (Figure 5). Sequence S40 encompasses the lower part of the Kareem Formation and is underlain by the T30 "terrace" (erosional unconformity, Figure 5).

Sequence S40 is overlain by the T40 terrace, which represents a third-order MFS with a condensed section deposited in an open-marine environment (Ramzy et al., 1996). However, this MFS was never observed in the field (Ramzy et al., 1996; Dolson et al. 1996). The T40 terrace is overlain by sequence S50, coinciding with the upper part of the Kareem Formation. The T50 terrace above represents an unconformable SB and forms the base to the Belayim Formation. Thus, the Kareem Formation was interpreted as a single transgressive-regressive cycle (transgressive systems tract followed by highstand systems tract) by Dolson et al. (1996). In contrast, we interpret two third-order sequences KS1 and KS2 in the Kareem Formation, which are described from base to top in the following sections.

### **Kareem Sequence 1 (KS1)**

#### ***Lower Boundary of Kareem Sequence 1 (SB1)***

The base of KS1 is Sequence Boundary 1 (SB1), a regional unconformity between the Kareem Formation and underlying Rudeis Formation (Patton et al., 1994; Bosworth, 1995; Bosworth and McClay, 2001). The abrupt decrease in GR at this surface is related to the basal anhydrite of the Kareem Formation, which overlies distal marine shale of the Rudeis Formation. SB1 reflects a rapid change in the environment of deposition triggered by a decrease in relative sea level (Underhill and Partington, 1993, 1994). The submarine expression of SB1 is an erosion surface below the early LST1 deposits (Figure 4). In the WSB, SB1 marks the boundary between a retrogradational ("dirtying-upward") log motif of the upper part of the Rudeis Formation to an aggradational to progradational ("cleaning-upward") log motif of LST1 (Figure 4). SB1 can not be followed to the southernmost part of the WSB (at the S. Ras El-Ush-1 well), due to a fault cut (Figure 4).



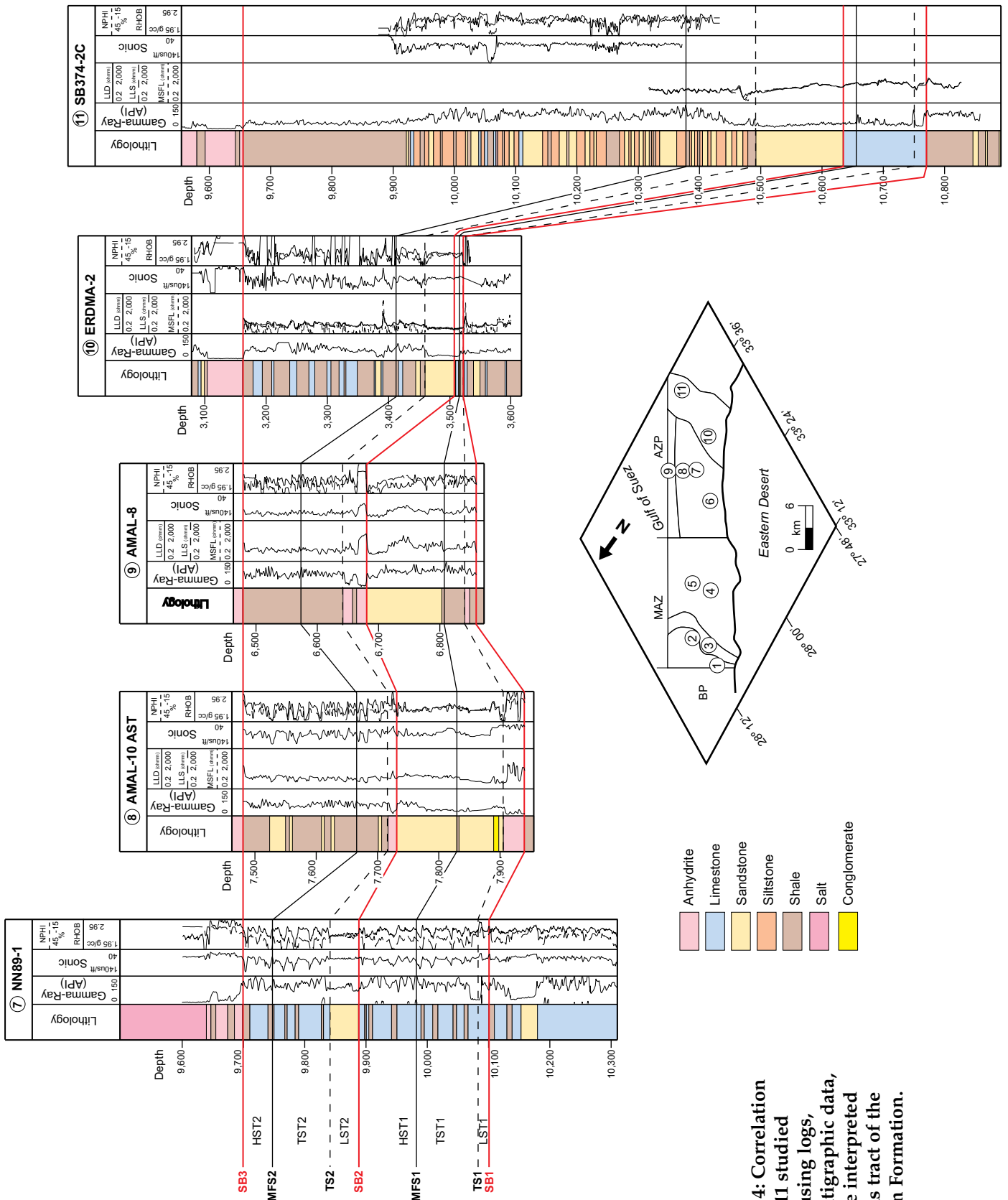


**Figure 4: Correlation of the 11 studied wells using logs, biostratigraphic data, and the interpreted systems tract of the Kareem Formation.**

**Lowstand Systems Tract of Kareem Sequence 1 (LST1)**

LST1 sediments are characterized by low GR, relatively high resistivity, low velocity, high to low density, and moderate to low neutron associated with decreasing PFA (Figure 5). Apart from the wells on FB V in the southern part of the WSB, sediments of the LST1 are present throughout the WSB. Argillaceous limestones and shales with few sandstones occur in the basin center and the southern parts of the MAZ (Morgan Accommodation Zone) on FB II and FB III (at the ERDMA-1, GB84-6 and GS334-2 wells, Figure 8). The lithology changes to anhydrites at FB I in the northern part of the MAZ (at the GC84-14 and LL87-3 wells) and at FB IV south of this zone (at the NN88-1, NN89-1, and Amal-10 AST wells, Figure 8). In the southernmost part of the WSB on FB VI (at the S. Ras El-Ush-1 and W. Ashrafi-1X wells, Figure 8) the LST1 sediments are represented by argillaceous limestones. Thickness of LST1 ranges between 1 ft at NN88-1 and 43 ft at Amal-10AST (Figure 4).

Age	Stage	Formation	Sequences	System tracts	Thickness (ft)	Lithology	Log trends	PFA and B/P trends	Depositional environments	Major sequences in the G.O.S.	
Middle Miocene	Langhian	Kareem	SB3	KS1	HST2	30-722	Calcareous shale, argillaceous limestone and sandstone of less polymictic clasts, Fe-oxides and carbonate cement. Few siltstone.	Decreasing GR (cleaning-upward), moderate to low resistivity and high moderate velocity. Moderate to low density and high to moderate neutron.	Decreasing PFA and increasing B/P ratio.	Middle neritic to upper bathyal	T50 S50
					TST2	45-153	Calcareous shale and argillaceous limestone intercalations. Few siltstone and sandstone of less polymictic clasts, Fe-oxides and carbonate cement.	Increasing GR (dirtying-upward), moderate to low resistivity and velocity. Moderate to low density and high to moderate neutron.	Increasing PFA and decreasing B/P ratio.	Middle-outer neritic to upper bathyal	T40
					LST2	14-432	Mainly sandstone of polymictic clasts, mica flakes, Fe-oxides and carbonate cement. Shale and argillaceous cherty limestone.	Blocky or box car high GR, relatively high resistivity and low velocity. Moderate to low density and high to moderate neutron.	Abrupt decrease in PFA and increase in B/P ratio.	Local restricted lagoons to upper bathyal	
			SB2	KS1	HST1	5-128	Calcareous shale and argillaceous limestone intercalations. Sandstone of polymictic clasts, Fe-oxides and carbonate cement.	Decreasing GR (cleaning – upward), moderate to low resistivity and velocity. Moderate to low density and high to moderate neutron.	Decreasing PFA and increasing B/P ratio.	Middle neritic to upper bathyal	S40
					TST1	5-98	Mainly calcareous shale with argillaceous limestone and sandstone of polymictic clasts, Fe-oxides and carbonate cement.	Increasing GR (cleaning - upward), moderate to low resistivity and high to moderate velocity. High to moderate density and neutron.	Increasing PFA and decreasing B/P ratio.	Middle-outer neritic to upper bathyal	
					LST1	1-43	Mainly anhydrite with argillaceous limestone, shale and few sandstone.	Blocky or box car high GR, high resistivity and low velocity. High to moderate density and moderate to low neutron.	Abrupt decrease in PFA and increase in B/P ratio.	Local restricted lagoons to upper bathyal	
			SB1	KS1	LST1	1-43	Mainly anhydrite with argillaceous limestone, shale and few sandstone.	Blocky or box car high GR, high resistivity and low velocity. High to moderate density and moderate to low neutron.	Abrupt decrease in PFA and increase in B/P ratio.	Local restricted lagoons to upper bathyal	T30

Figure 5: Petrographic, log, and micropaleontologic characteristics, with accompanying interpretation, for all systems tract of the two third-order sequences (KS1 and KS2) of the Kareem Formation. Our interpretation is compared to previously described sequences (S40 and S50) in the Gulf of Suez (after Dolson et al., 1996; Ramzy et al., 1996; Krebs et al., 1997).



**Interpretation of Lowstand Systems Tract of Kareem Sequence 1 (LST1)**

LST1 sediments deposited in portions of the WSB reflect relative sea-level fall that outpaced subsidence. The appearance of the first Middle Miocene evaporites (on structurally elevated FB I and FB IV, Figure 8a) at the base of the Kareem Formation, denotes an abrupt facies change from deep-marine shale of the Rudeis Formation to a restricted lagoon in the southwestern part of the Gulf basin (Dolson et al., 1996; Bosworth and McClay, 2001). In contrast, during deposition of LST1 sediments in FB II and FB III in the MAZ and FB VI in the southernmost part of the WSB (Figure 8a), subsidence rates apparently outpaced the fall in relative sea level resulting in deposition of mainly deep-marine shales on FB III and hemi-pelagic carbonate sediments on FB II and FB VI (see also Winn et al., 2001; Carr et al., 2003; Jackson et al., 2005; Khalil and McClay, 2008).

Rare terrigenous sediments, deposited in the MAZ on FB III (Figure 8a), may indicate fluvial processes, resulting from discharge of small amounts of detritus from elevated Proterozoic and pre-Miocene footwall blocks along the western rift shoulder (see also Gawthorpe et al., 1994; Salah and Alsharhan, 1997; Young et al., 2000; Winn et al., 2001; Jackson et al., 2005). The thin and nearly uniform thickness of the LST1 sediments along the WSB indicates minor subsidence rates (Jackson et al., 2005). Thickness variations along FB IV (Figure 6) indicate block rotation down to the southeast during deposition of LST1 (Figure 8a). Similar relations between thickness variations and directions of fault block rotations were described in the Gulf of Suez (Winn et al., 2001) and the eastern Atlasic Domain of Algeria (Herkat and Guiraud, 2006).

**Transgressive Surface of Kareem Sequence 1 (TS1)**

This surface separates the aggradational to progradational LST1 deposits from the overlying retrograding interval of TST1 (TS1, Figure 4). TS1 is marked by high GR and PFA and likely represents the onset of transgression and rising sea level, and may have been associated with erosion by high wave or tide energy in near-shore to inner-shelf environments.

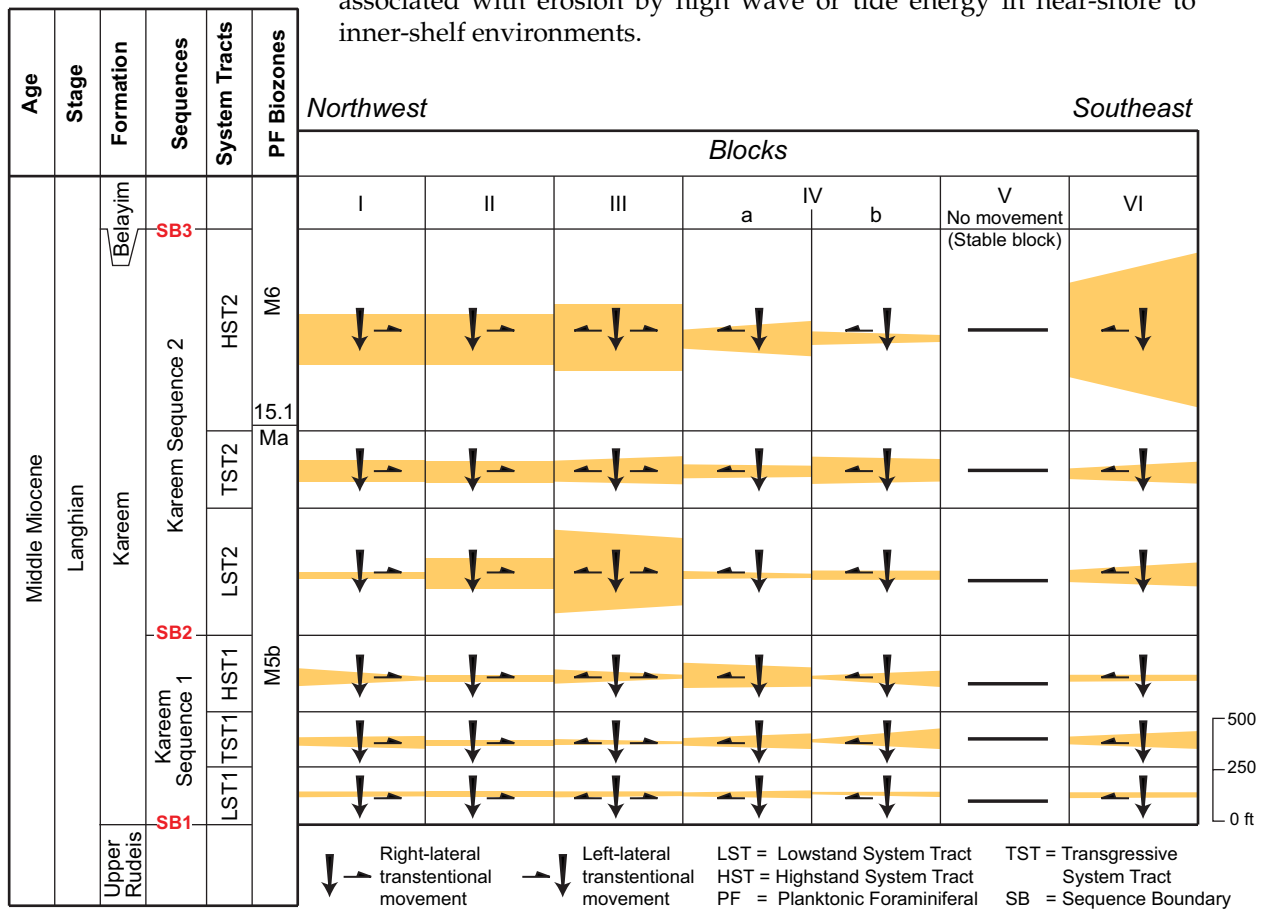
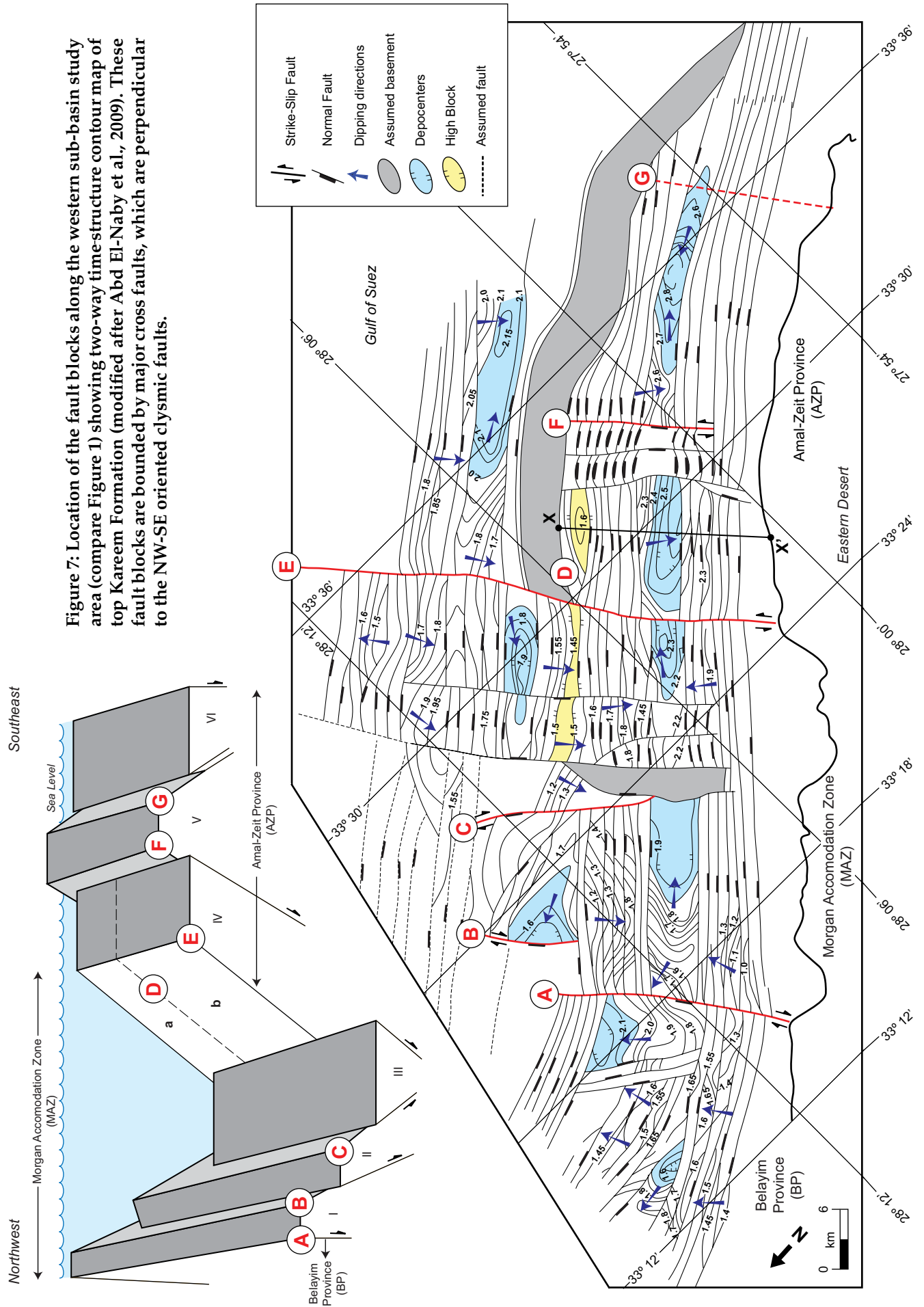


**Figure 6: Tectonic movements (arrows) and thickness variations of each fault block (gray shaded areas) for the systems tract of the Kareem Formation. The sizes of the arrows are directly proportional to the subsidence rates.**



### Transgressive Systems Tract of Kareem Sequence 1 (TST1)

The retrogradational TST1 sediments are characterized by an upward increase in GR (“dirtying-upward”), moderate to low resistivity, high to moderate velocity, and high to moderate density and neutron (Figure 5). These sediments also are marked by an upward increase in PFA and decreasing B/P ratios. Lithologically these sediments are mainly calcareous shales deposited on FB I in the MAZ (at the GC84-14 and LL87-3 wells, Figure 9), argillaceous limestones deposited on FB II in the MAZ (at the ERDMA-1 well) and FB IVb and FB VI in the AZP (at the NN88-1, NN89-1, S. Ras El-Ush-1, and W. Ashrafi-1X wells), and mainly shales with few argillaceous limestones on FB III in the MAZ (at the GB84-6 and GS334-2 wells, Figure 9). In FB IVa of the AZP (at the Amal-10AST well, Figure 9), TST1 sediments are composed of sandstones (facies type A, Figure 3) and fine conglomerates at the base. Sand grains are subrounded to angular and composed mainly of quartz, feldspar, granite, carbonate and shale (see also Kandeel, 2008). The thickness of TST1 is quite variable (from 5 ft at GS334-2 to 98 ft at NN89-1, Figure 4).

### Interpretation of Transgressive Systems Tract of Kareem Sequence 1 (TST1)

Log response and lithofacies characteristics of TST1 sediments along portions of the WSB indicate an upward-finining and upward-deepening succession into more distal and shale-rich marine sediments. These likely were deposited during rising sea level and imply a decrease in depositional energy. These sediments may have been deposited in low-energy, middle- to outer-neritic to upper-bathyal environments, when the rate of sea-level rise exceeded the subsidence rate and the formation of accommodation space outpaced the rate of sediment supply (Jackson et al., 2005). The TST1 sediments are characterized by the presence of hemipelagic carbonates on FB II (in the MAZ), FB VI (in the AZP) and FB IVb (Figure 9a). The low B/P ratio and the very high PFA of these deposits indicate the incursion of a well-oxygenated, open-marine environment, following the evaporitic phase of LST1 (Dolson et al., 1996).

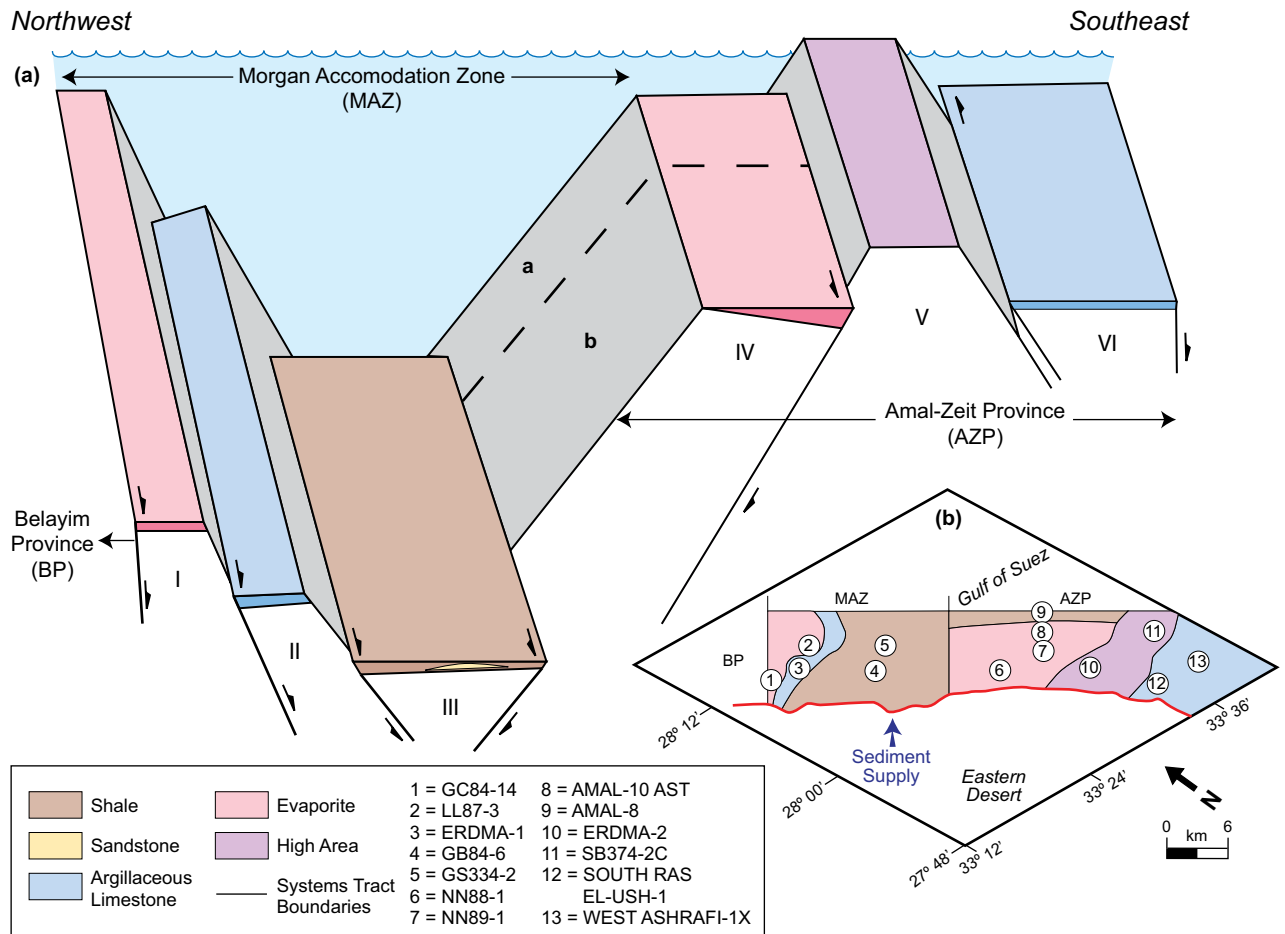


**Figure 8: Tectono-sedimentary model (a) and lithofacies distribution map (b) for lowstand systems tract 1 (LST1) of the Kareem Formation.**

In contrast, polymictic clasts within pebbly sandstones (facies type A, Figure 3) and conglomerates occur on FB IVa, indicating sediment influx along a major drainage system. Frequent slumping occurred, with detritus derived from elevated Proterozoic and pre-Miocene footwall blocks along the western rift shoulder. The drainage system extended along the elevated FB V and fed a prograding fan delta on FB IVa (Figure 9a). This block was structurally higher and subsided less than FB IVb during deposition of TST1. The absence of fan delta sediments on FB IVb reflects a drainage system centered on an east-dipping FB V (Figure 9). Similar structurally controlled deposition of syn-rift coarse-grained fan-delta systems is described from the eastern margin of the Gulf of Suez (Gawthorpe et al., 1990; Gupta et al., 1999), northern margin of the Gulf of Suez (Young et al., 2000; Jackson et al., 2005), northwestern margin of the Red Sea margin (Khalil and McClay, 2008), and Gulf of Corinth (Dart et al., 1994).

During lower rates of relative sea-level rise the sediment supply was greater than the rate of generation of new accommodation space at FB IVa, resulting in progradation of the delta on this block to the northwest (Figure 9). However, during rapid relative sea-level rise the sediment supply was unable to keep up with the increasing accommodation space, resulting in abandonment and transgression across the fan. Thickness patterns along FB I, FB IVa, FB IVb, and FB VI (Figure 6) indicate that these fault blocks rotated down to the southeast, whereas thickness trends along FB III reveal that this block rotated down to the northwest during deposition of TST1 (compare to Herkat and Guiraud, 2006, Figure 9).

### Maximum Flooding Surface of Kareem Sequence 1 (MFS1)

A maximum flooding surface (MFS1) separates deposits of the retrograding interval of TST1 below from the prograding deposits of HST1 above (Figure 4). This surface (including the TST1 sediments below) is associated with high values in GR and PFA.

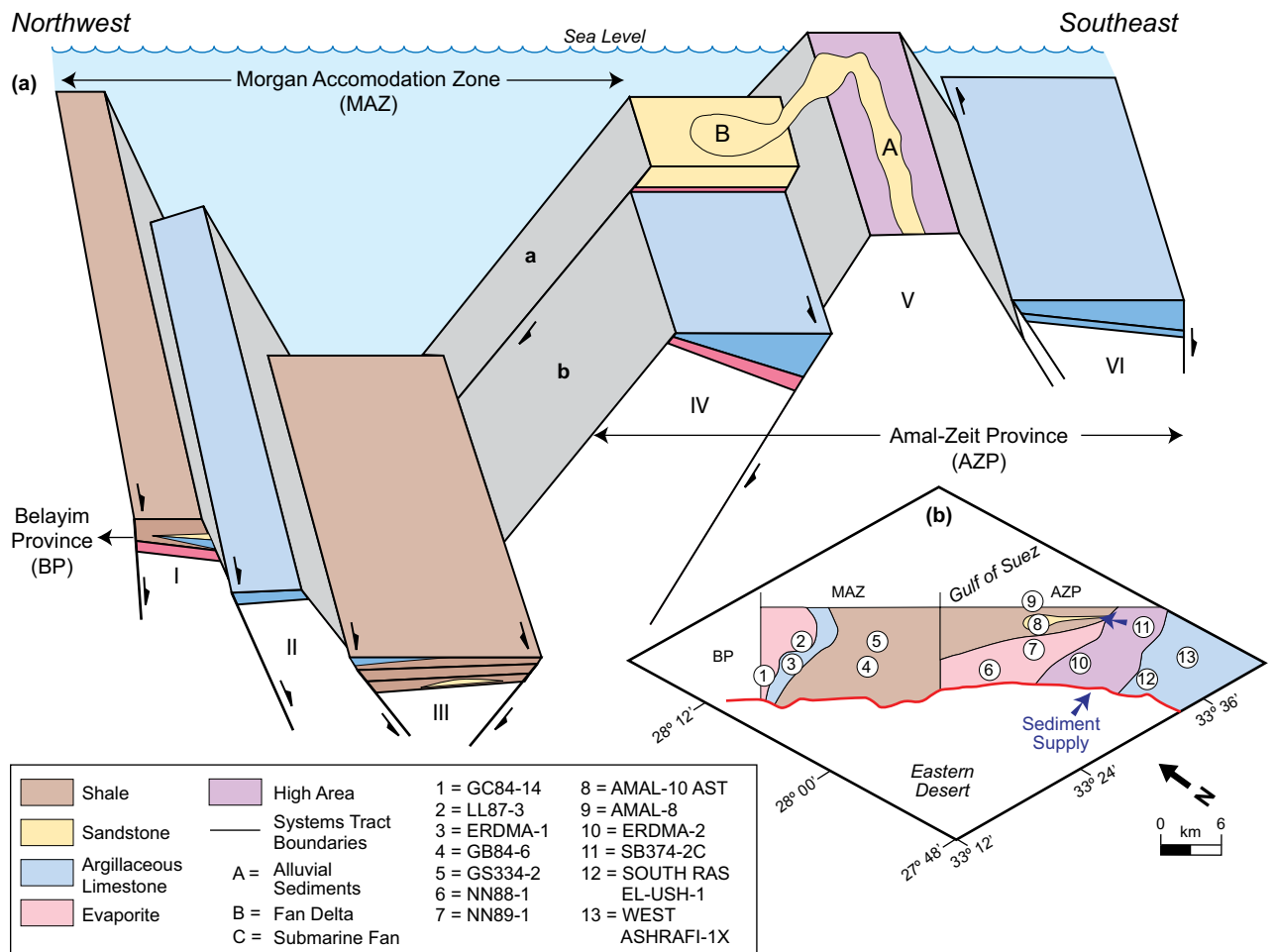


Figure 9: Tectono-sedimentary model (a) and lithofacies distribution map (b) for transgressive systems tract 1 (TST1) of the Kareem Formation.

### Highstand Systems Tract of Kareem Sequence 1 (HST1)

The progradational HST1 sediments are characterized by an upward decrease in GR (“cleaning-upward”), moderate to low resistivity and velocity, moderate to low density, and high to moderate neutron readings (Figure 5). These sediments also exhibit an upward decrease in PFA and increase in B/P ratio. Lithofacies of the HST1 are similar to TST1 (Figure 10). However, the HST1 sediments contain coarser grained sandstones (facies type A, Figure 3) with higher clast content on FB IVa in the AZP (at the Amal-10AST and Amal-8 wells, Figure 10). Thickness of HST1 varies from 5 ft at Ras El-Ush-1 to 128 ft at Amal-8 (Figure 4).

### Interpretation of Highstand Systems Tract of Kareem Sequence 1 (HST1)

Lithofacies, paleontological, and progradational features of HST1 indicate a gradual regression with increasing terrigenous influx and transport during major river floods through drainage systems along FB V. As a consequence, a second fan-delta lobe evolved on FB IVa towards the northwest when the rate of sediment supply exceeded the rate of new accommodation space created by rising relative sea level (Figure 10). The abundance of conglomerate clasts and the coarsening of sandstones (facies type A) reflect increasing depositional energy and high-energy density flows, coupled with decreasing water depths (Young et al., 2000). Compared with the high influx of fan-delta sediments on FB IVa, few terrigenous sediments were deposited on FB III (in the MAZ, Figure 10a). The terrigenous sediments on FB III and FB IVa reflect the progressive unroofing of the uplifted Proterozoic and pre-Miocene footwall blocks along the western rift shoulder. At the same time, hemipelagic carbonates accumulated on FB II, FB IVb, and FB VI (Figure 10) and indicate middle-neritic to upper-bathyal deposition.

Thickness variations along FB I, FB III, and FB IVa (Figure 6) reveal that these blocks rotated down to the northwest, whereas thickness patterns along FB IVb reflect that this block rotated down to the southeast during deposition of HST1 sediments (Figure 10a). HST1 is limited upward by the second sequence boundary (SB2) which caps Kareem sequence 1 (Figure 4).

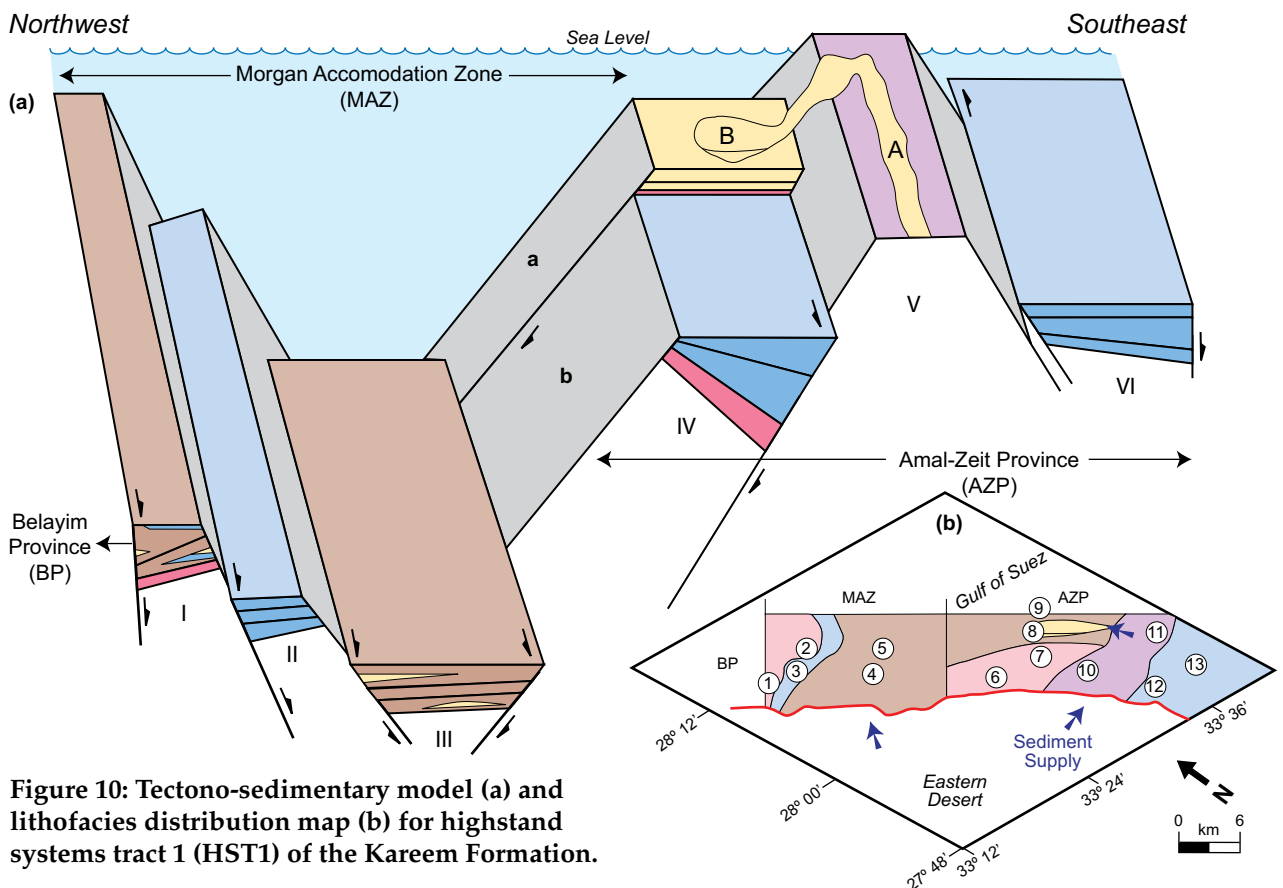


Figure 10: Tectono-sedimentary model (a) and lithofacies distribution map (b) for highstand systems tract 1 (HST1) of the Kareem Formation.

## Kareem Sequence 2 (KS2)

### *Lower Boundary of Kareem Sequence 2 (SB2)*

The base of KS2 is delineated by Sequence Boundary 2 (SB2). This surface is marked by an abrupt decrease in GR and PFA, which may imply an abrupt jump to a shallower water facies during rapid lowering of relative sea level. This surface also marks an upward change from a progradational (“cleaning-upward”) log motif of HST1 deposits to an aggradational log motif of the overlying LST2 deposits (Figure 4).

### *Lowstand Systems Tract of Kareem Sequence 2 (LST2)*

The aggradational LST2 sediments have quite similar log characteristics to those of LST1 (Figure 5), with dominantly sandstones (facies types A and B, Figure 3) deposited on FB I, FB II, FB IVb, and FB IV (at the GC84-14, LL87-3, ERDMA-1, NN88-1, NN89-1, S. Ras El-Ush-1, and W. Ashrafi-1X wells, Figure 11). Sandstones, shales, and argillaceous cherty limestones characterize sedimentation on FB III (at the GB84-6 and GS334-2 wells), while anhydrites were deposited on FB IVa (at the Amal-10AST and Amal-8 wells, Figure 11). The thickness of LST2 changes from 14 ft at Amal-10AST to 432 ft at GB84-6 (Figure 4).

### *Interpretation of Lowstand Systems Tract of Kareem Sequence 2 (LST2)*

The sandstones (facies types A and B) and polymictic conglomerate clasts as well as mica in the LST2 sediments demonstrate high terrigenous influx in the WSB. The drainage systems experienced frequent slumping with abundant detritus likely supplied from the same source as sediments of LST1 (Figure 11b). These drainage systems fed prograding fan deltas during LST2 on the structurally high FB I and FB II (in the MAZ) and FB IVb and FB VI (in the AZP, compare Gawthorpe et al., 1994; Salah and Alsharhan, 1997; Young et al., 2000). The role of antecedent drainage systems in focusing deposition of coarse-grained sediments is well known from similar rift basins, e.g. Gulf of Corinth (Seeger and Alexander, 1993), Gulf of Suez (Gawthorpe et al., 1990; McClay et al., 1998; Gupta et al., 1999; Leppard and Gawthorpe, 2006), and the eastern Atlasic Domain of Algeria (Herkat and Guiraud, 2006).

LST2 received sediment also from turbidity currents beyond the shelf edge where accommodation was greater on structurally low FB III in the MAZ (compare to Young et al., 2000; Winn et al., 2001, Figure 11). This turbidity formed submarine fans composed of small clasts and fine-grained sandstones (facies type B, Figure 3). These clast-rich turbidites reflect an increase in depositional energy coupled with decreasing water depths (compare Young et al., 2000). Deposition of deep-marine carbonates in the upper part of LST2, on structurally low FB III in the MAZ (at the GB84-6 well, Figure 11b), was relatively short-lived. The carbonates may have developed during a break in siliciclastic deposition or lateral to the main clastic entry point. The carbonates were locally re-worked when sand was subsequently transported across them, possibly due to delta channel or lobe switching or sudden sediment input during seasonal fluvial flooding. Deposition of deep-marine pelagic shales during late LST2 on the structurally low FB III may reflect the cessation of siliciclastic deposition (Figure 11a). Furthermore, the presence of large amounts of Fe-oxides in this portion of LST2 may indicate deposition in an oxidizing environment (Salah and Alsharhan, 1997).

FB IVa represented an elevated ridge with weak subsidence rates during KS1; the deposition of fan deltas resulted in a progressive reduction in water depth and evaporate sedimentation (compare Herkat and Guiraud, 2006, Figure 11a). On FB I and FB II in the MAZ, sediment supply exceeded subsidence rates and resulted in the deposition of fan-delta sediments on both fault blocks with greater thickness on the structurally deeper FB II. At the end of LST2 accumulation on the two fault blocks was balanced and, as a consequence, both fault blocks (I and II) reacted during future intervals as one (Figure 11a). The great thickness of LST2 sediments on FB III implies high sediment supply (Figure 6) coupled with high subsidence rates. Thickness variations along FB III (Figure 6) indicate rotation down to the northwest (similar to FB IVa), whereas thickness variations along FB VI reflect a rotation down to the southeast.

### *Transgressive Surface of Kareem Sequence 2 (TS2)*

The upper boundary of LST2 is marked by an abrupt increase in GR which delineates the TS2 surface (Figure 4). TS2 represents the onset of a major sea-level rise that may have been associated with transgressive erosion.

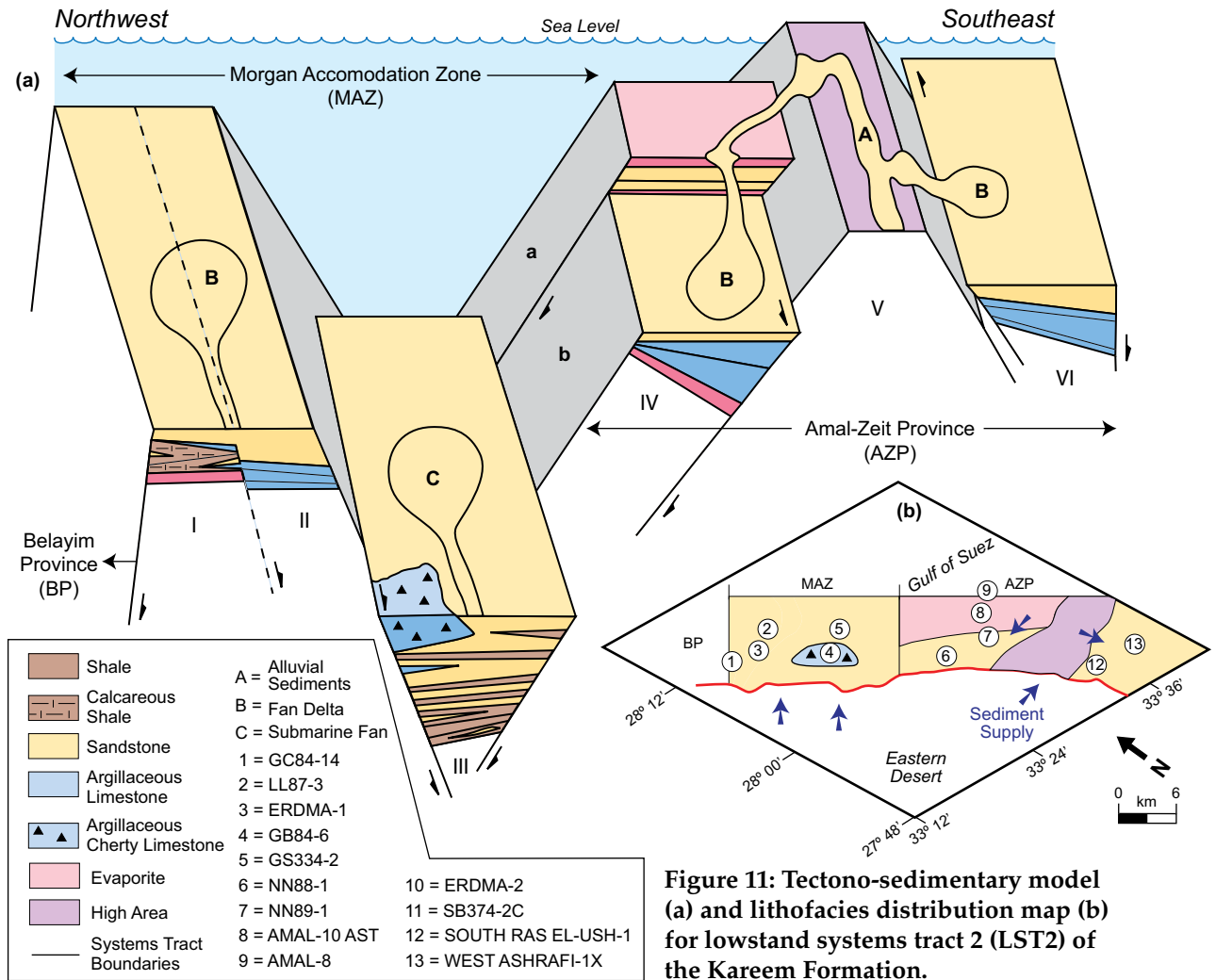


**Figure 11: Tectono-sedimentary model (a) and lithofacies distribution map (b) for lowstand systems tract 2 (LST2) of the Kareem Formation.**

### ***Transgressive Systems Tract of Kareem Sequence 2 (TST2)***

TST2 sediments have quite similar lithologic and log characteristics to those of TST1. TST2 sediments are mainly calcareous shales with few sandstones and argillaceous limestone intercalations on FB I, FB II, and FB IVa (at the GC84-14, LL87-3, ERDMA-1, Amal-10AST and Amal-8 wells); mainly shales with sandstones and few limestone intercalations on FB III (at the GB84-6 and GS334-2 wells); and argillaceous limestones with few sandstones on FB IVb (at the NN88-1 and NN89-1 wells, Figure 12). Sandstones (facies type B, Figure 3), siltstones, shales, and few limestone intercalations accumulated on FB VI (at S. Ras El-Ush-1 and W. Ashrafi-1X) at the southernmost part of the WSB (Figure 12). The thickness of TST2 varies from 45 ft at S. Ras El-Ush-1 to 153 ft at NN 88-1 (Figure 4).

### ***Interpretation of Transgressive Systems Tract of Kareem Sequence 2 (TST2)***

The log motif and lithologic properties of TST2 along the WSB indicate repeated upward-fining and upward-deepening retrogradational parasequences composed mainly of distal, shale-rich, marine sediments. The frequent occurrence of planktonic foraminifer and nannofossils in these sediments indicate low-energy middle- to outer-neritic to upper-bathyal depositional settings. In contrast to TST1, hemipelagic carbonates are only recorded on FB IVb (Figure 12).

Pebbly sandstones (facies type B, Figure 3), with polymictic clasts, siltstones, and shales (rich in planktonic foraminifer and nannofossils) intercalations on FB VI reflect deposition of a submarine fan associated with high subsidence rates (Figure 12a). The source of this submarine fan, like during LST2, was detritus derived from the elevated Proterozoic and pre-Miocene footwall blocks along the western rift shoulder. Drainage systems extended along the elevated FB V above sea level and fed submarine fans that prograded to the southeast (Figure 12a). Progradation of the submarine fans

indicates that sediment supply was greater than the rate of newly generated accommodation space at FB VI. However, sediment supply was unable to keep up with accommodation development across the fan at FB VI resulting in abandonment and transgression (compare Young et al., 2000; Herkat and Guiraud, 2006). Generally, the “dirtying-upward” GR of TST2 (Figure 4) may be a result of a decrease in sand percentage in thinly bedded turbidites, and so may record the abandonment of submarine-fan deposition.

Compared to the high influx of submarine-fan sediments, little terrigenous material was deposited on FB I, FB II, and FB III (in the MAZ) and on FB IVa and FB IVb (in the AZP) via the drainage systems on FB V (Figure 12). The nonmarine units indicate a return to fluvial processes and to progressive unroofing of the uplifted Proterozoic and pre-Miocene footwall blocks along the western rift shoulder. FB IVa is characterized by higher subsidence rates than FB IVb during TST2 deposition. This difference led to deep-marine pelagic shale with higher planktonic foraminiferal abundance on FB IVa, in contrast to hemipelagic carbonates on FB IVb (Figure 12a). The movement of FB IVa marks an inversion of the subsidence compared with the deposition of preceding system tracts (Herkat and Guiraud, 2006). Thickness variations of TST2 along FB III and FB VI (Figure 6) indicate that these blocks rotated down to the southeast, whereas thickness variations along FB IVb reveal that this block rotated down to the northwest.

**Maximum Flooding Surface of Kareem Sequence 2 (MFS2)**

MFS2 delineates the upper boundary of the retrogradational succession TST2. The surface is marked by maximum GR response and PFA (Figure 4). It may coincide with the T40 terrace of Ramzy et al. (1996). MFS2 is overlain by the prograding interval of HST2.

**Highstand Systems Tract of Kareem Sequence 2 (HST2)**

HST2 sediments have very similar log features to those of HST1 (Figure 5). Moreover, they show similar lithologic characteristics as TST2 sediments, with mainly sandstones (facies type B, Figure 3),

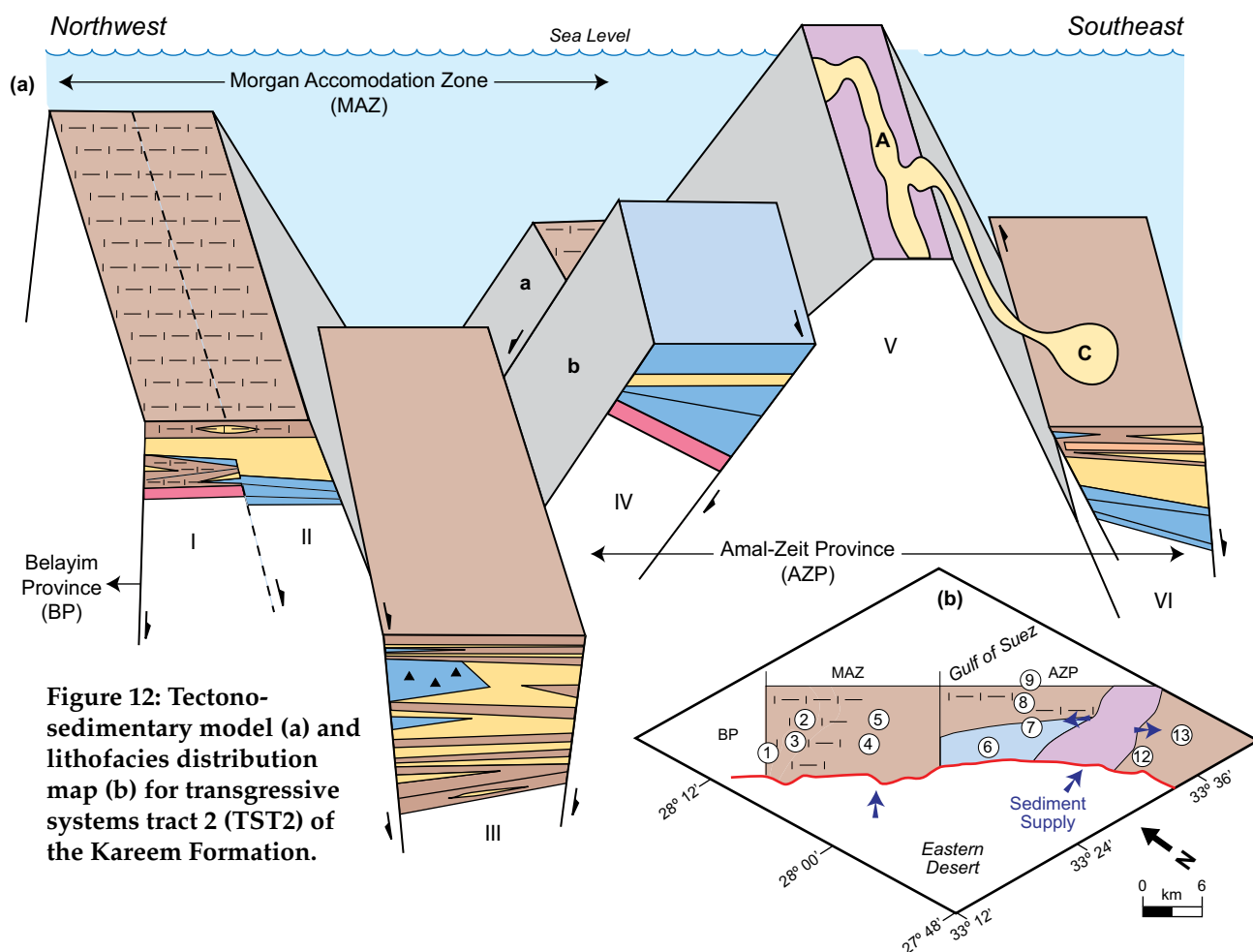


**Figure 12: Tectono-sedimentary model (a) and lithofacies distribution map (b) for transgressive systems tract 2 (TST2) of the Kareem Formation.**



shales, and few limestone intercalations deposited on FB III (at the GB84-6 and GS334-2 wells, Figure 13). The sandstones contain clasts that are smaller in size than those of TST2. The thickness of HST2 is quite variable (ranging between 30 ft at NN89-1 and 722 ft at W. Ashrafi-1X, Figure 4).

**Interpretation Highstand Systems Tract of Kareem Sequence 2 (HST2)**

The coarsening- or sandying-upward pattern of HST2 reflects a decelerating relative sea-level rise and return to terrigenous sedimentation across the shelf. A submarine fan was deposited during this interval on FB VI (Figure 13a). With its southeasterly directed progradation, we assume a similar source as for the TST2 submarine fans (Figure 13). The large thickness of HST2 (Figure 6) on FB VI indicates high subsidence rates of this fault block. Furthermore, submarine-fan progradation suggests that sediment supply exceeded the rate of new accommodation space at FB VI. At the same time, hemipelagic carbonate sediments accumulated on FB IVb (Figure 13a).

Another submarine fan formed on FB III (Figure 13a) with a similar source of terrigenous material as submarine fan deposited during LST2. On the other hand, smaller clast sizes may indicate minor fluvial discharge (Young et al., 2000). This fan's large thickness (Figure 6) reflects deposition coupled with high subsidence rates of this fault block. Similar to TST2, only thin terrigenous sediments were deposited on FB I and FB II (in the MAZ) or FB IVa and FB IVb (in the AZP). Thickness variations along FB IVa and FB VI (Figure 6) indicate that these blocks rotated down to the southeast, whereas isopach patterns along FB IVb reveal that this block rotated down to the northwest.

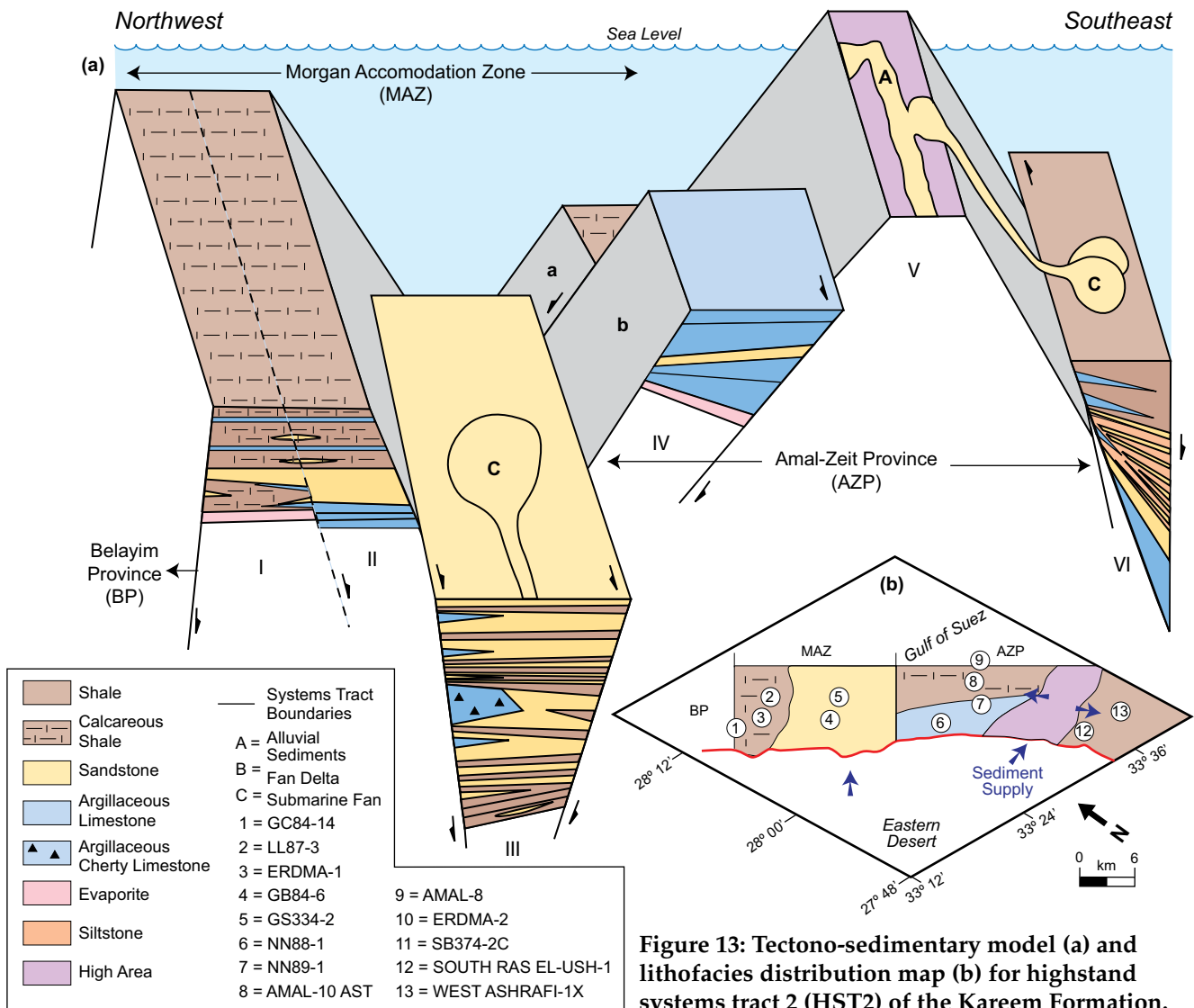


**Figure 13: Tectono-sedimentary model (a) and lithofacies distribution map (b) for highstand systems tract 2 (HST2) of the Kareem Formation.**

### ***Upper Boundary of Kareem Sequence 2 (SB2)***

The upper limit of HST2 is determined by a third sequence boundary SB3 (Figure 4) which is marked by an abrupt decrease in GR. It coincides with the T50 terrace (Figure 5), a major unconformity in the Gulf of Suez (Dolson et al., 1996; Ramzy et al., 1996; Krebs et al., 1997).

## **DISCUSSION AND CONCLUSIONS**

Complex interaction between eustasy and tectonism apparently controlled the depositional processes and sequence development of the Middle Miocene (Langhian) Kareem Formation in the NW-SE oriented extensional WSB. The complicated structural and depositional history with abrupt thickness and facies changes, deep basins, high relief, and differential fault-block movements is similar to structural and depositional complexity recorded elsewhere in the Gulf of Suez rift (e.g., Burchette, 1987; Schütz, 1994; Winn et al., 2001), the coastal Red Sea (e.g., Montenat et al., 1988; Gawthorpe et al., 1990; Purser et al., 1990; Khalil and McClay, 2006), the central North Sea basin (Bishop et al., 1995), the north-eastern Gulf of Mexico (Wu et al., 1990), Central Greece Gulf basins (e.g., Gulf of Corinth and Gulf of Evvia, Gawthorpe et al., 1994) and other continental rifts (e.g., Gawthorpe and Hurst, 1993). The Kareem Formation in the study area can be subdivided into two third-order sequences based on the identification of key chronostratigraphic surfaces and system tracts.

The depositional models we propose for the syn-rift sediments of the various systems tracts of both sequences indicate a strong tectonic influence controlling subsidence of the individual fault blocks along the WSB during the "mid-Clysmic" or "mid-Rudeis" event (Patton et al., 1994). This event caused a rejuvenation of basement faults, which resulted in abrupt thickness and facies changes coupled with rotation of the different fault blocks during deposition of the Kareem Formation. The high dip angle of the faults ( $> 60^\circ$ ) along the WSB created steep topographic and bathymetric gradients and development of depositional systems with a discrete shelf-slope break along the western rift shoulder (compare Gawthorpe et al., 1994). Our tectono-sedimentary models might be applied to other rift basins where pre-existing basement structures have exerted a strong control on rift-fault geometries and patterns.

Most of the systems tracts are preserved as complete successions with larger thicknesses in the Morgan Accommodation Zone (MAZ), because major transfer (accommodation) zones commonly represent footwall topographic lows. Hence, the accommodation zone acts as a focus for increasing volumes of sediment entering rifts (compare Leeder and Gawthorpe, 1987; Morely et al., 1990; Gawthorpe et al., 1994; Jackson et al., 2005). Overall, the rate of subsidence of the hangingwall and resulting accommodation development, coupled with high rate of sediment supply, exceeded the rate of relative sea-level fall during deposition of the Kareem Formation.

Compared with the first Kareem sequence (KS1), subsidence rates of the second Kareem sequence (KS2) were significantly larger as indicated by larger thicknesses and deposition of a large number of thick fan deltas and submarine fans (mainly on FB III and FB VI). These thick deposits may reflect increased sediment supply due to wet climates during the Middle Miocene (Perrin et al., 1998; Mader et al., 2004).

The submarine fans apparently originated from drainage systems that experienced frequent slumping. Abundant detritus was derived from the elevated Proterozoic and pre-Miocene footwall blocks along the western rift shoulder. The drainage systems also yielded thin fluvial sandstones on the structurally elevated FB V (above sea level) at the ERDMA-2 well. This sandstone can not be placed into one of the defined systems tracts due to its reduced thickness, which also makes it difficult to differentiate from the underlying Rudeis Formation. Moreover, strong fluvial influx on the structurally high FB V resulted in the erosion of Early to Middle Miocene sediments (early Kareem, Rudeis and Nukhul formations) in the Amal-Zeit Province (AZP) at the SB374-2C well.

Within our sequence stratigraphic framework, the interaction between tectonism and sedimentation of the syn-rift Kareem Formation becomes more obvious and allows highlighting the paleotectonic history. Despite the depositional complexity, small-scale fault block by fault block facies interpretation allows delineating tectonically influenced sedimentation processes. Our tectono-sedimentary models

could be used for facies-predictions in the other parts of the extensional Gulf of Suez rift basin to clarify the poor understanding of interacting tectonism and sedimentation.

## ACKNOWLEDGEMENTS

We are deeply indebted to Dr. Christian Scheibner, Geochronology Department, Bremen University (Germany) for fruitful discussion and careful revision of an earlier version of the manuscript. We also thank RWE DEA AG Petroleum Company, Hamburg, Germany, for various software support. We wish to express our gratitude to the Egyptian General Petroleum Corporation (EGPC) for releasing the log data. We would like to extend our special thanks to our colleagues of the Geochronology working group in Bremen University for various help. The two anonymous reviewers are also thanked for their valuable comments and suggestions. The drafting and design of the paper by Nestor A. Buhay II is much appreciated.

## REFERENCES

- Abd El-Naby, A., M. Abd El-Aal, J. Kuss, M. Boukhary and A. Lashin 2009. Structural and basin evolution in Miocene time, southwestern Gulf of Suez, Egypt. *Neues Jahrbuch für Geologie und Paläontologie – Abhandlungen*, v. 251, no. 3, p. 331-353.
- Armentrout, J.M. and J.F. Clement 1990. Biostratigraphic calibration of depositional cycles: a case study in High Island-Galveston-East Breaks, offshore Texas. In *Sequence stratigraphy as an exploration Tool, concepts and practices in the Gulf Coast*. SEPM, Gulf Coast Section, Eleventh Annual Research Conference, Program with Abstracts, p. 21-51.
- Beleity, A.M. 1984. The composite standard and definition of paleoevents in the Gulf of Suez: Egyptian General Petroleum Corporation, Sixth Exploration Conference, p. 181-198.
- Bishop, D.J., P.G. Buchanan and C.J. Bishop 1995. Gravity-driven thin-skinned extension above Zechstein Group evaporites in the western central North Sea: an application of computer-aided section restoration techniques. *Marine and Petroleum Geology*, v. 12, p. 115-135.
- Bosworth, W. 1995. A high-strain rift model for the southern Gulf of Suez, Egypt. In J.J. Lambiasi (Ed.), *Hydrocarbon habitat in rift basins*. Geological Society, London, special publication no. 80, p. 75-112.
- Bosworth, W. and K. McClay 2001. Structural and stratigraphic evolution of the Gulf of Suez Rift, Egypt: a synthesis. In P.A. Ziegler, W. Cavazza, A.H.F. Robertson and S. Crasquin-Soleau (Eds.), *Peri-Tethys Memoir 6: Peri-Tethyan rift/wrench basins and passive margins*. Museum National d'Histoire naturelle de Paris, *Memoirs*, v. 186, p. 567-606.
- Burchette, T.P. 1987. Tectonic control on carbonate platform facies distribution and sequence stratigraphy: Miocene, Gulf of Suez. *Sedimentary Geology*, v. 59, p. 179-204.
- Carr, I.D., R.L. Gawthorpe, C.A.L. Jackson, I.R. Sharp and A. Sadek 2003. Sedimentology and sequence stratigraphy of early syn-rift tidal sediments: The Nukhul Formation, Suez Rift, Egypt. *Journal of sedimentary research*, v. 73, p. 407-421.
- Dart, C.J., R.E.L. Collier, R.L. Gawthorpe, J.V. Keller and G. Nichols 1994. Sequence stratigraphy of (?) Pliocene-Quaternary syn-rift Gilbert type deltas, northern Peloponnesos, Greece. *Marine and Petroleum Geology*, v. 11, p. 545-560.
- Dolson, J., O. El Gendi, H. Charmy, M. Fathalla and I. Gaafar 1996. Gulf of Suez rift basin sequence models – Part A. Miocene sequence stratigraphy and exploration significance in the Greater October field area, northern Gulf of Suez. In Egyptian General Petroleum Corporation. Thirteen Exploration Conference, Cairo, Egypt, v. 2, p. 227-241.
- Emery, D. and K. Myers 1996. *Sequence stratigraphy*. Blackwell Science. Ltd., Oxford, 297 p.
- Gawthorpe, R. L. and J.M. Hurst 1993. Transfer zones in extensional basins: their structural style and influence in drainage development and stratigraphy. *Journal of the Geological Society*, v. 150, p. 1137-1152.
- Gawthorpe, R.L. and M.R. Leeder 2000. Tectono-sedimentary evolution of active extensional basins. *Basin Research*, v. 12, p. 195-218.
- Gawthorpe, R.L., J.M. Hurst and C.P. Sladen 1990. Evolution of Miocene footwall derived coarse-grained deltas. Gulf of Suez, Egypt: implications for exploration. *Bulletin of the American Association of Petroleum Geologists*, v. 74, p. 1077-1086.
- Gawthorpe, R.L., A.J. Fraser and E. L.I. Collier 1994. Sequence stratigraphy in active extensional basins: implications for the interpretation of ancient basin-fills, *Marine and Petroleum Geology*, v. 11, no. 6, p. 642-658.

- Gupta, S., J.R. Underhill, I.R. Sharp and R.L. Gawthorpe 1999. Role of fault interactions in controlling synrift sediment dispersal patterns: Miocene Abu Alaqa Group. Suez Rift, Sinai, Egypt. *Basin Research*, v. 11, p. 167-189.
- Hardy, S., C.J. Dart and D. Waltham 1994. Computer modelling of the influence of tectonics on sequence architecture of coarse-grained fan deltas. *Marine and Petroleum Geology*, v. 11, p. 561-574.
- Herkat, M. and R. Guiraud 2006. The relationships between tectonics and sedimentation in the Late Cretaceous series of the eastern Atlasic Domain (Algeria). *Journal of African Earth Sciences*. v. 46, p. 346-370.
- Jackson, C.A.L., R.L. Gawthorpe, I.D. Carr and I.R. Sharp 2005. Normal faulting as a control on the stratigraphic development of shallow marine syn-rift sequences: the Nukhul and Lower Rudeis Formations, Hammam Faraun fault block, Suez Rift, Egypt. *Sedimentology*, v. 52, p. 313-338.
- Kandeel, A.A.E. 2008. Geological modeling and reservoir characterization of Kareem Formation in Amal oil field, south Gulf of Suez. Unpublished MSc thesis, Cairo University, Cairo, Egypt, 252 p.
- Khalil, S.M. and K.R. McClay 2008. Structural control on syn-rift sedimentation, northwest Red Sea Margin, Egypt. *Marine and Petroleum Geology*, v. 26, p. 1018-1034.
- Krebs, W.N., D. Wescott, I. Nummedahl, G. Gaafar, G. Azazi and S. Karamat 1997. Graphic correlation and sequence stratigraphy of Neogene rocks in the Gulf of Suez. In *Fauna, flora and sequence stratigraphy*. Association Paleontologie Francaise de Stratigraphie, v. 168, no. 1, p. 64-71.
- Leeder, M.R. and R.L. Gawthorpe 1987. Sedimentary models for extensional tilt-block/half-graben basins. In M.P. Coward, J.F. Dewey and P.L. Hancock (Eds.), *Continental extensional tectonics*. Geological Society of London Special Publication No. 28, p. 139-152.
- Leeder, M.R., R.E. Li. Collier, A.L.H. Aziz, M. Trout, G. Ferentinos, G. Papatheodorou and E. Lyberis 2002. Tectono-sedimentary processes along an active marine/lacustrine half-graben margin: Alkyonides gulf. Gulf of Corinth, Greece. *Basin Research*, v. 14, p. 25-41.
- Leppard, C.W. and R.L. Gawthorpe 2006. Sedimentology of rift climax deep water systems; Lower Rudeis Formation, Hammam Faraun fault block, Suez Rift, Egypt. *Sedimentary Geology*. v. 191, p. 67-87.
- Mader, D., L. Cleaveland, D.M. Bice, A. Montanari and C. Koeberl 2004. High-resolution cyclostratigraphic analysis of multiple climate proxies from a short Langhian pelagic succession in the Conero Riviera, Ancona (Italy). *Palaeogeography, palaeoclimatology, palaeoecology*, v. 211, p. 325-344.
- McClay, K.R., G. J. Nichols, S. Khalil, M. Darwish and W. Bosworth 1998. Extensional tectonics and sedimentation, eastern Gulf of Suez. Egypt. In B.H. Purser and D.W.J. Bosence (Eds.), *Sedimentation and tectonics of rift basins, Red Sea-Gulf of Aden*: Chapman and Hall, London, p. 223-238.
- Mitchum, R.M. Jr., J.B. Sangree, P.R. Vail and W.W. Wornardt 1993. Recognizing sequences and systems tracts from well logs, seismic data, and biostratigraphy: examples from the late Cenozoic. In P. Weimer and H.W. Posamentier (Eds.), *Siliciclastic sequence stratigraphy. Recent developments and applications*. American Association of Petroleum Geologists, Memoir No. 58, p. 163-197.
- Montenat, C., P. Ott D'estevou, B. Purser, P.F. Burollet, J.-J. Jarrige, F. Orszag-Sperber, E. Philobos, J.-C. Plaziat, P. Prat, J.-P. Richert, N. Roussel and J.-P. Thiriet 1988. Tectonic and sedimentary evolution of the Gulf of Suez and the northwestern Red Sea. *Tectonophysics*, v. 153, p. 161-177.
- Morely, C.K., R.A. Nelson, T.L. Patton and S.G. Munn 1990. Transfer zones in the East Africa rift system and their relevance to hydrocarbon exploration in rifts. *Bulletin of the American Association of Petroleum Geologists*, v. 74, p. 1234-1253.
- Nummedal, D. and D.J.P. Swift 1987. Transgressive stratigraphy at sequence bounding unconformities: some principles derived from Holocene and Cretaceous examples. In D. Nummedal, O.H. Pilkey and J.D. Howard (Eds.), *Sea level fluctuations and coastal evolution*. Society Economic Paleontology Mineralogy Special Publication No. 41, p. 241-260.
- Patton, T.L., A.R. Moustafa, R.A. Nelson and S.A. Abdine 1994. Tectonic evolution and structural setting of the Suez Rift. In S.M. London (Ed.), *Interior rift basins*. American Association of Petroleum Geologists Memoir No. 59, p. 7-55.
- Perrin, C., J.C. Plaziat and B.R. Rosen 1998. Miocene coral reefs and reef corals of the south-western Gulf of Suez and north-western Red Sea: distribution, diversity and regional environmental controls. In B.H. Purser and D.W.J. Bosence (Eds.), *Sedimentation and tectonics of rift basins: Red Sea-Gulf of Aden*. Chapman and Hall, London, p. 296-320.

- Posamentier, H.W. and G.P. Allen 1999. Siliciclastic sequence stratigraphy - concepts and applications. SEPM concepts in Sedimentology and Paleontology, no. 7, Tulsa, Oklahoma, USA, 204 p.
- Purser, B.H., E.R. Philobos and M. Soliman 1990. Sedimentation and rifting in the NW parts of the Red Sea: a review. Bulletin de la Societe Geologique de France, v. 6, p. 371-384.
- Ramzy, M., B. Steer, F. Abu-Shadi, M. Schlorholtz, J. Mika, J. Dolson and M. Zinger 1996. Gulf of Suez basin sequence models - Part B. Miocene sequence stratigraphy and exploration significance in the central and the southern Gulf of Suez. In Egyptian general petroleum corporation. Thirteen Exploration Conference, Cairo, Egypt, v. 2, p. 242-256.
- Rider, M. 2004. The geological interpretation of well logs. Second Edition, Sutherland, Scotland, 280 p.
- Salah, M.G. and A.S. Alsharhan 1997. The Miocene Kareem Formation in the southern Gulf of Suez, Egypt: a review on stratigraphy and petroleum geology. Journal of Petroleum Geology, v. 20, no. 3, p. 327-346.
- Schaffer, B. L. 1987. The potential of calcareous nannofossils for recognizing Plio-Pleistocene climatic cycles and sequence boundaries on the shelf: Gulf Coast Section SEPM Foundation, Eighth Annual Research Conference, p. 142-145.
- Schlumberger 1995. Well evaluation conference – Egypt; Houston, Texas, U.S.A, 87p.
- Seger, M.J. and J. Alexander 1993. Distribution of Plio-Pleistocene and modern coarse-grained deltas south of the Gulf of Corinth, Greece. In L. Frostick and R. Steel (Eds.), Tectonic controls and signatures in sedimentary successions. International Association of Sedimentologists, special publication no. 20, p. 37-48.
- Schütz, K.I. 1994. Structure and stratigraphy of the Gulf of Suez, Egypt. In S. M. Landon (Ed.), Interior rift basins. American Association of Petroleum Geologists Memoir No. 59, p. 57-96.
- Underhill, J.R. and M.A. Partington 1993. Jurassic thermal doming and deflation in the North Sea: implications of the sequence stratigraphic evidence. In J.R. Parker (Ed.), Petroleum geology of northwest Europe, Proceedings Fourth Conference, p. 337-346.
- Underhill, J.R. and M.A. Partington 1994. Use of genetic sequence stratigraphy in defining and determining a regional tectonic control on the “Mid-Cimmerian Unconformity” implications for North Sea basin development and the global sea level chart. In P. Weimer and H. W. Posamentier (Eds.), 1993, Siliciclastic sequence stratigraphy, recent developments and applications. American Association of Petroleum Geologists Memoir no. 58, p. 449-484.
- Wescott, W. A., W. N. Krebs, J. Dolson, S. A. Karamat and D. Nummedahl 1996. Rift basin sequence stratigraphy: some examples from the Gulf of Suez. GeoArabia, v. 1, no. 2, p. 343-358.
- Winn, R.D., P.D. Crevello and W. Bosworth 2001. Lower Miocene Nukhul Formation, Gebel el Zeit, Egypt: Model for structural control on early synrift strata and reservoirs, Gulf of Suez. Bulletin of the American Association of Petroleum Geologists, v. 85, no. 10, p. 1871-1890.
- Wu, S.A. W. Bally and C. Cramez 1990. Allochthonous salt, structure and stratigraphy of the north-eastern Gulf of Mexico. Part II: structure. Marine and Petroleum Geology, v. 7, p. 334-370.
- Young, M.J., R.L. Gawthorpe and I.R. Sharp 2000. Sedimentology and sequence stratigraphy of a transfer zone coarse-grained delta, Miocene Suez Rift, Egypt. Sedimentology, v. 47, p. 1081-1104.

## ABOUT THE AUTHORS

**Ahmed I.M. Abd El-Naby** obtained a PhD in 2009 from Ain Shams University. He was a member in the project entitled “a field geologic study of southwestern Sinai for development” During 1999-2002. Ahmed had a scholarship from the Egyptian Mission Department to Bremen University in Bremen, Germany, during the academic years 2007-2009, to carry out research on sequence stratigraphy under supervision of Professor Jochen Kuss. He got also an internship from DEA RWE Oil Company from November 2008 to January 2009. He has published two articles in Neues Jahrbuch and Geologia Croatica.

[zowail2000@yahoo.com](mailto:zowail2000@yahoo.com)



**Hussam Ghanem** is currently working towards his PhD in Geochronology at Bremen University. His research is focused on stratigraphy evolution of carbonate platform (Cretaceous of Syria) and the interpretation of Syrian tectonic history through Sedimentary analysis. He obtained a MSc in Geology and worked for a short time with Petro- service Syria.

[hussam\\_ghanem@yahoo.com](mailto:hussam_ghanem@yahoo.com)



**Mohamed Boukhary** obtained a PhD in 1973 from Ain Shams University. He was a fellow at Marie Curie University in Paris, France, during the academic year 1979-1980, where he worked on the research field of larger foraminifera (Nummulitacea) with Dr. Alphonse Blondeau. Mohamed served as Assistant Professor of Stratigraphy and Micropaleontology at Qatar University from 1981 to 1985 and in 1987 he became a Professor of Micropaleontology. He joined United Arab Emirates University in 1993, and became Chairman of the Geology Department between 1996 and 1998. Mohamed has been Chairman of the Geology Department at Ain Shams University from 2003 to 2007.

[moboukhary@yahoo.com](mailto:moboukhary@yahoo.com)



**Mohamed H. Abdel Aal** obtained a PhD in 1988 from Ain Shams University. He was a fellow at School of Geology and Geophysics Oklahoma University, USA, from February to October 1997, where he worked on the research field of Seismic Stratigraphy and amplitude versus offset (AVO). Mohamed served as Assistant Professor of Geophysics at Ain Shams University from 1994 to 2000 and in 2001 he became a Professor of Geophysics. He has been Vice Dean of Post graduate studies and researches at Faculty of education, Ain Shams University from 2005 up till now.

[mabdelaal81@yahoo.com](mailto:mabdelaal81@yahoo.com)



**Sebastian Lüning** obtained his Geology/Palaeontology diploma from the University of Göttingen, Germany, in 1994 working on stratigraphy and terrane movements in northwest Thailand. He is a Senior Geologist with RWE Dea since 2007. His interest in North Africa and Arabia began in 1994 when he commenced a study about Late Cretaceous – Lower Tertiary strata of the Sinai Peninsula. He received his PhD in Geology in 1997 from the University of Bremen, Germany. Between 1997–2000 he was a post-doctoral Fellow at the University of Wales, Aberystwyth, and the Royal Holloway University of London, sponsored and based at the oil company LASMO plc, London. Here, he carried out and co-ordinated a variety of projects, including a re-evaluation of the petroleum potential of the Kufra Basin (southeast Libya) and North Africa-wide studies about structural styles and Silurian and Frasnian 'hot' shales. Since 2000 he is continuing his black shale studies as a post-doctoral Fellow at the University of Bremen, sponsored by the German Science Foundation (DFG) and the petroleum-industry supported North Africa Research Group (NARG). Sebastian has been operating the geoscience platforms [www.northafrica.de](http://www.northafrica.de) and [www.blackshale.com](http://www.blackshale.com) since 2001.

[sebastian.luening@rwe.com](mailto:sebastian.luening@rwe.com)



**Jochen Kuss** was awarded a PhD in 1983 by Erlangen University in Germany following studies on Upper Triassic ramp deposits in the northern Calcareous Alps. From 1983 to 1991 he was an Assistant Professor at the Technical University of Berlin and undertook sedimentologic and stratigraphic work in Egypt and Jordan. In 1991 Jochen joined the University of Bremen. His main research interests are field work-based studies of marine Cretaceous to Paleogene successions in North Africa and the Middle East. Methods used include petrography, (micro) biostratigraphy, geochemistry, remote sensing and basin modeling.

[kuss@uni-bremen.de](mailto:kuss@uni-bremen.de)

